Chemical mass balance equations for open-system magma chamber processes under equilibrium crystallization conditions

Koshi NISIHMURA*

Abstract

A mass balance model is developed to describe the behavior of trace elements and isotopes during open-system magma chamber processes under equilibrium crystallization conditions. The model incorporates the effects of melt influx (recharge or mixing), equilibrium crystallization, magma extraction, assimilation of anatectic wall-rock melt, and partial settling of crystals. The analytical solution of the mass-balance differential equations gives a quantitative account of the evolution of trace elements and isotopes. The chemical trends of the magma differ markedly from those predicted by a recently developed open-system magma chamber model under disequilibrium crystallization (crystal zoning) conditions. These two end-member models provide the upper and lower limits for the compositional variations expected during open-system magma chamber processes under natural conditions.

Keywords: open-system magmatic process, geochemical modeling, crystal isotope stratigraphy, Sr isotopes, mamga chamber

1. Introduction

Recent remarkable advances in micro-analytical techniques have revealed that isotopic variations recorded from core to rim of a single mineral grain reflect progressive changes in the composition of the liquid from which the mineral crystallized (e.g., Feldstein et al., 1994; Davidson and Tepley, 1997; Davidson et al., 1998, 2001, 2007; Knesel et al., 1999; Tepley et al., 1999, 2000; Waight et al., 2000; Ramos et al., 2005; Charlier et al., 2006, 2008). Consequently, isotope ratios of the liquid and of integrated (bulk) crystals are inevitably different in an open-system magma chamber. Nishimura (2019) recently developed a geochemical model that describes the chemical zoning of

* Natural Science Laboratory, Toyo University, 5-28-20 Hakusan, Bunkyo-ku, Tokyo 112-8606, Japan

crystals in an open-system magma chamber, assuming that each increment of crystal growth perfectly seals off the previous zone and prevents it from re-equilibrating with the evolving liquid. However, chemical gradients that define crystal zoning are rarely perfectly stable, and they tend to destabilize due to the kinetic process of diffusion (e.g., Costa et al., 2003, 2010; Saunders et al., 2010; Druitt et al., 2012; Moore et al., 2014; Till et al., 2015; Singer et al., 2016). This study seeks to develop a mass balance model for perfect equilibrium crystallization in an open-system magma chamber as a model representing an end-member scenario to complement the model proposed by Nishimura (2019).

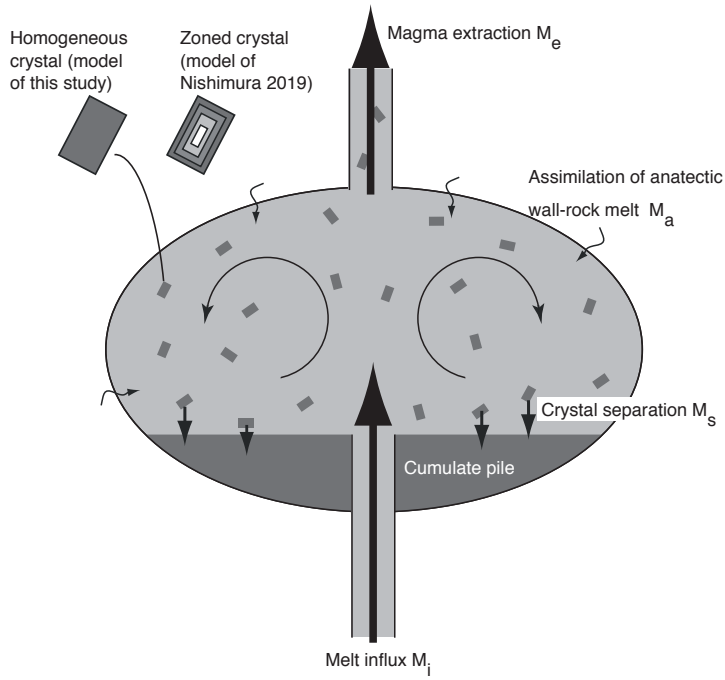

Fig. 1 : Schematic illustration of an open-system magma chamber model incorporating the effects of simultaneous melt influx (subscript 'i' in the figure) (recharge or mixing), equilibrium crystallization, magma extraction (e), assimilation (a), and the partial settling (s) of crystals. M = Mass; subscripts indicate the applicable process.

2. Model

This study develops a geochemical model for equilibrium crystallization in an open-system magma chamber, following the method of Nishimura (2019). Figure 1 is a schematic illustration of open-system magma chamber processes, including melt influx (recharge or mixing), the growth of homogeneous crystals, magma extraction,

assimilation of anatectic wall-rock melt, and partial settling of crystals. Crystals are assumed to be homogeneously distributed by vigorous convection in a magma chamber. The extracted (erupted) magma is therefore composed of liquid and suspended crystals. The crystals are partially segregated from the magma body to the cumulate pile at the base of the magma chamber due to gravity, even if the convective velocity is much greater than the crystal settling velocity (Martin and Nokes, 1988). The mass balance differential equations for an element's concentration and its isotopic ratio in the magma can be respectively expressed as

$$\dot{M}_a C_a + \dot{M}_i C_i - \dot{M}_s D C_l - \dot{M}_e C_m = C_m \frac{dM_m}{dt} + M_m \frac{dC_m}{dt}\ , \qquad (1)$$

$$\dot{M}_a C_a \varepsilon_a + \dot{M}_i C_i \varepsilon_i - \dot{M}_s D C_l \varepsilon_l - \dot{M}_e C_m \varepsilon_m = C_m \varepsilon_m \frac{dM_m}{dt} + M_m \varepsilon_m \frac{dC_m}{dt} + C_m M_m \frac{d\varepsilon_m}{dt}\ , \qquad (2)$$

where $\dot{M}_a$ is the mass assimilation rate (mass/unit time), C_a is the element's concentration in the melt (liquid) derived from wall-rock melting, $\dot{M}_i$ is the mass influx rate (mass/unit time), C_i is the element's concentration in the injected liquid, D is the bulk crystal/liquid partition coefficient for the element, C_l is the element's concentration in the liquid in the magma chamber, $\dot{M}_e$ is the mass extraction rate (mass/unit time), ϕ is the weight fraction of the suspended crystals in the magma chamber relative to the total mass of magma, M_l is the mass of the liquid in the magma chamber, ε_a is the isotope ratio of the wall-rock, ε_i is the isotope ratio of the injected liquid, ε l is the isotope ratio of the liquid in the magma chamber, and $\dot{M}_s$ is the rate of gravitational separation of crystals from magma (mass/unit time) (see Table 1). Fractional crystallization due to gravitational crystal settling is imperfect if a certain proportion of crystals is suspended for a duration that is sufficient to enable re-equilibration with the surrounding liquid (Fig. 1). This case is based on the assumption that equilibrium is always maintained between the liquid and the suspended crystals. The trace element concentration in the liquid can therefore be expressed as follows:

$$C_l = \frac{C_m}{1 - \phi + \phi D}. \qquad (3)$$

The isotopic ratio in the crystallizing phases is assumed to always be the same as that of the magma. Incorporating Eq. (3) into Eqs. (1) and (2), the mass balance differential equations for an element's concentration in a magma and the isotopic ratio of that magma can be respectively rewritten as

$$\dot{M}_a C_a + \dot{M}_i C_i - \dot{M}_s D^* C_m - \dot{M}_e C_m = C_m \frac{dM_m}{dt} + M_m \frac{dC_m}{dt}\ , \qquad (4)$$

and

$$\dot{M}_a C_a \varepsilon_a + \dot{M}_i C_i \varepsilon_i - \dot{M}_s D^* C_m \varepsilon_m - \dot{M}_e C_m \varepsilon_m = C_m \varepsilon_m \frac{dM_m}{dt} + M_m \varepsilon_m \frac{dC_m}{dt} + C_m M_m \frac{d\varepsilon_m}{dt}, \quad (5)$$

where D^* is the effective distribution coefficient (O'Hara, 1993; O'Hara and Fry, 1996; Nishimura, 2009), which can be expressed as

$$D^* = \frac{D}{1 - \phi + \phi D}. \quad (6)$$

DePaolo (1981) defined the constant ratio of the rate of assimilation to the rate of crystal separation ($r_a = \dot{M}_a / \dot{M}_s$) in order to analytically solve the differential equations for simultaneous assimilation and fractional crystallization (AFC). Similarly, this study defines the constant ratio of the rate of liquid influx to the rate of crystal separation ($r_i = \dot{M}_i / \dot{M}_s$) and that of the rate of magma (liquid + suspended crystals) extraction to the rate of crystal separation ($r_e = \dot{M}_e / \dot{M}_s$). It should be noted that the ratios r_a, r_i, and r_e can vary during the open-system evolution of a magma body; e.g., Bohrson and Spera (2001) reported temporal variations in ra. However, these constant ratios could be used for approximation, at least for a short crystallization period, and could be estimated from the variation trends of trace elements and isotopes, as was done for the AFC model (e.g., Powell, 1984; Mantovani and Hawkesworth, 1990; Young et al., 1992; Aitcheson and Forrest, 1994; Roberts and Clemens, 1995; Caffe et al., 2002). The instantaneous rate of change in the mass of a magma body, affected simultaneously by assimilation, liquid magma influx, magma (liquid + suspended crystals) extraction, and gravitational separation of crystals, is given as

$$\frac{dM_m}{dt} = (r_a + r_i - r_e - 1)\dot{M}_s, \quad (7)$$

where M_m is the mass of the magma body. When $r_a + r_i - r_e = 1$ (i.e., $\dot{M}_a + \dot{M}_i = \dot{M}_s + \dot{M}_e$), added material (assimilant + injected liquid) is balanced by an equivalent mass of subtracted material (gravitationally segregated crystals + extracted magma), meaning that the magma mass remains constant. The analytical solutions to the system of differential equations (Eqs. 3 and 4) for an element can be separated conveniently into two cases: one for $r_a + r_i - r_e \neq 1$, and another for $r_a + r_i - r_e = 1$. Assuming that ϕ, D, C_a, ε_a, C_i, and ε_i are constant, the solutions can be written as follows:

For $r_a + r_i - r_e \neq 1$ (general case),

$$C_m = j/k + (C_m^0 - j/k) F_m^{-k}, \quad (8)$$

and

$$\varepsilon_m = \frac{l + (kC_m^0\varepsilon_m^0 - l)F_m^{-k}}{j + (kC_m^0 - j)F_m^{-k}}, \quad (9)$$

where C_l^0 is the initial concentration of the element in the liquid, ε_l^0 is the initial isotope ratio of the liquid, C_x^0 is the initial concentration of the element in the suspended crystals, ε_x^0 is the initial isotope ratio of the suspended crystals, F_m is the ratio of magma mass to the initial magma mass ($F_m \equiv M_m/M_m^0$), and

$$j = \frac{r_a C_a + r_i C_i}{r_a + r_i - r_e - 1}, \quad (10)$$

$$k = \frac{D^* + r_e}{r_a + r_i - r_e - 1} + 1, \quad (11)$$

$$l = \frac{r_a C_a \varepsilon_a + r_i C_i \varepsilon_i}{r_a + r_i - r_e - 1}. \quad (12)$$

For $r_a + r_i - r_e = 1$,

$$C_m = \frac{m}{n} + e^{-n\frac{M_s}{M_m}}\left(C_m^0 - \frac{m}{n}\right), \quad (13)$$

and

$$\varepsilon_m = \left[\frac{o}{n} + e^{-n\frac{M_s}{M_m}}\left(C_m^0\varepsilon_m^0 - \frac{o}{n}\right)\right]/C_m, \quad (14)$$

where

$$M_s = \int_0^t \dot{M}_s\, dt, \quad (15)$$

$$m = r_a C_a + r_i C_i, \quad (16)$$

$$n = D^* + r_e, \quad (17)$$

and

$$o = r_a C_a \varepsilon_a + r_i C_i \varepsilon_i. \quad (18)$$

Table 1 : Symbols used in the formulation

Symbol	Description	Unit
$\dot{M}_a$	Rate of assimilation of anatectic wall-rock melt	kg s^{-1}
$\dot{M}_i$	Rate of liquid influx (recharge or mixing)	kg s^{-1}
$\dot{M}_e$	Rate of magma extraction	kg s^{-1}
$\dot{M}_s$	Rate of crystal separation from magma by gravitational settling	kg s^{-1}
r_a	Ratio of rate of assimilation to rate of crystal separation	
r_i	Ratio of rate of liquid influx to rate of crystal separation	
r_e	Ratio of rate of magma extraction to rate of crystal separation	
M_l	Mass of liquid in magma body	kg
M_m	Mass of magma (liquid + suspended crystals)	kg
M_m^0	Mass of initial magma	kg
M_s	Total mass of crystals separated from the magma by gravitational settling	kg
ϕ	Weight fraction of suspended crystals relative to total magma mass	
F_m	Ratio of magma mass to initial magma mass	
C_a	Trace element concentration of anatectic melt (assimilant)	ppmw
C_i	Trace element concentration of injected liquid	ppmw
C_l	Trace element concentration of liquid in magma body	ppmw
C_m	Trace element concentration of magma	ppmw
C_m^0	Trace element concentration of initial magma	ppmw
D	Bulk crystal/liquid partition coefficient	ppmw
ε_a	Isotope ratio of anatectic wall-rock melt	
ε_i	Isotope ratio of injected liquid	
ε_l	Isotope ratio of liquid in magma body	
ε_m	Isotope ratio of magma	
ε_m^0	Isotope ratio of initial magma	
$j - o$	Constants defined in Eqs. 10–12 and 16–18	

3. Results

Figures 2 – 9 present examples of the evolution of the trace element concentration and isotope ratio ($^{87}Sr/^{86}Sr$) of the liquid, total suspended crystals, magma (whole rock), and crystal rims for several values of r_a, r_i r_e, and D. The results in the case of crystal zoning (Nishimura, 2019) are also shown for comparison (left panels in Figs. 2 – 9). The weight fraction of suspended crystals (ϕ) is assumed to be 0.2 for all cases. Under the assumption of constant ϕ, an increment of crystals greater than ϕ is separated from convecting magma to the cumulate pile throughout the crystallization process. The crystals being separated are assumed to have the same composition as those remaining in suspension. The relative trace element concentration of the anatectic wall-rock melt, normalized by that of the initial magma C_a/C_m^0, is assumed to be 0.25 for all cases. For simplicity, the recharged magma is assumed to have the same composition as the original unfractionated magma. The proportion of magma mass remaining (F_m) for $r_a + r_i -$

$r_e < 1$ decreases as the open-system process proceeds (Figs. 2 and 3), whereas F_m for $r_a + r_i - r_e > 1$ increases as the process proceeds (Figs. 4 and 5). This is because when $r_a + r_i - r_e < 1$ (i.e., $\dot{M}_a + \dot{M}_i < \dot{M}_s + \dot{M}_e$), the mass of added material (assimilant + injected liquid) is smaller than the mass of subtracted material (gravitationally separated crystals + extracted magma), meaning that the magma mass decreases, and when $r_a + r_i - r_e > 1$ (i.e., $\dot{M}_a + \dot{M}_i > \dot{M}_s + \dot{M}_e$), the mass of added material is greater than the mass of subtracted material, so the magma mass increases.

For the cases of both homogeneous and zoned crystals, and for a given compatible trace element (e.g., $D = 10$), the evolution paths of the bulk rock are strongly affected by suspended crystals and are therefore nearly parallel to those of the latter (Figs. 2 and 4). For an incompatible trace element (e.g., $D = 0.1$), the evolution paths of the bulk rock become similar to those of the liquid (Figs. 3 and 5). The results of simple fractional crystallization ($r_a = r_i = r_e = 0$) in the case of zoned crystals suspended in the liquid are compared with the results for homogeneous crystals (Figs. 2a and b; see also Nishimura, 2009). The homogenization (equilibration) of suspended crystals suppresses the depletion of compatible elements in liquid more effectively than in the zoned-crystal case. The compatible trace element concentrations of liquid, total suspended crystals, and whole rock decrease continuously with decreasing F_m (Fig. 2 a, b). When assimilation occurs and $r_a + r_i - r_e < 1$, the compatible trace element concentrations of liquid, total suspended crystals, and whole rock reach a compositional steady state (Fig. 2 c–h). In contrast, incompatible trace element concentrations never reach a steady state regardless of whether assimilation occurs (Fig. 3). When $r_a + r_i - r_e > 1$ and assimilation does occur, both compatible and incompatible elements attain a steady state (Figs. 4 and 5). In the case of no recharge and no extraction (Fig.2c, d), the evolution paths of liquid, total suspended crystals, and whole rock are identical to those obtained from the revised AFC (AIFC) model (Nishimura, 2012).

The addition of magma recharge affects the steady state concentrations of liquid, total suspended crystals, and whole rock (Fig. 2 e and f), whereas magma extraction does not (Fig. 2 g and h, Fig. 3 g and h). The value of D^{Sr} for tholeiitic-type basaltic magma may be much less than 1 unless plagioclase is the main crystallizing phase, in which case the value of D^{Sr} for silicic magma may be much larger than 1 because Sr enters sodic plagioclase and/or sanidine. The modeling results of $^{87}Sr/^{86}Sr$ variations for cases with $D^{Sr} = 0.1$ and $D^{Sr} = 10$ are shown in Figs. 4 and 5 to emphasize the difference between the trajectories for incompatible and compatible elements. The initial magma was assumed to have Sr = 400 ppm and $^{87}Sr/^{86}Sr = 0.7030$; the assimilant (anatectic wall-rock melt) was assumed to have Sr = 100 ppm and $^{87}Sr/^{86}Sr = 0.7200$. These values are identical to those in fig. 3 of DePaolo (1981).

When $D^{Sr} = 10$ and crystals are zoned, the $^{87}Sr/^{86}Sr$ paths of whole rock are close to those of total suspended crystals (left panels in Figs. 6 and 8), whereas when $D^{Sr} = 0.1$

and crystals are zoned, the $^{87}Sr/^{86}Sr$ paths of whole rock become almost identical to those of liquid or crystal rims (left panels in Figs. 7 and 9). When homogeneous crystals are grown under equilibrium conditions, the $^{87}Sr/^{86}Sr$ paths of whole rock, liquid, and suspended crystals are identical (right panels in Figs. 6 – 9). For both homogeneous and zoned crystal cases, and for $r_a + r_i - r_e < 1$, the $^{87}Sr/^{86}Sr$ ratios of liquid (or crystal rims), total suspended crystals, and whole rock reach steady states only when D^{Sr} is large (Figs. 6 and 7). For $r_a + r_i - r_e > 1$, the $^{87}Sr/^{86}Sr$ ratios of liquid (or crystal rim), total suspended crystals, and whole rock reach steady states regardless of the D^{Sr} value (Figs. 8 and 9).

The steady-state trace element concentrations and isotopic ratios of magma with homogeneous crystals for $r_a + r_i - r_e \neq 1$ can be expressed as

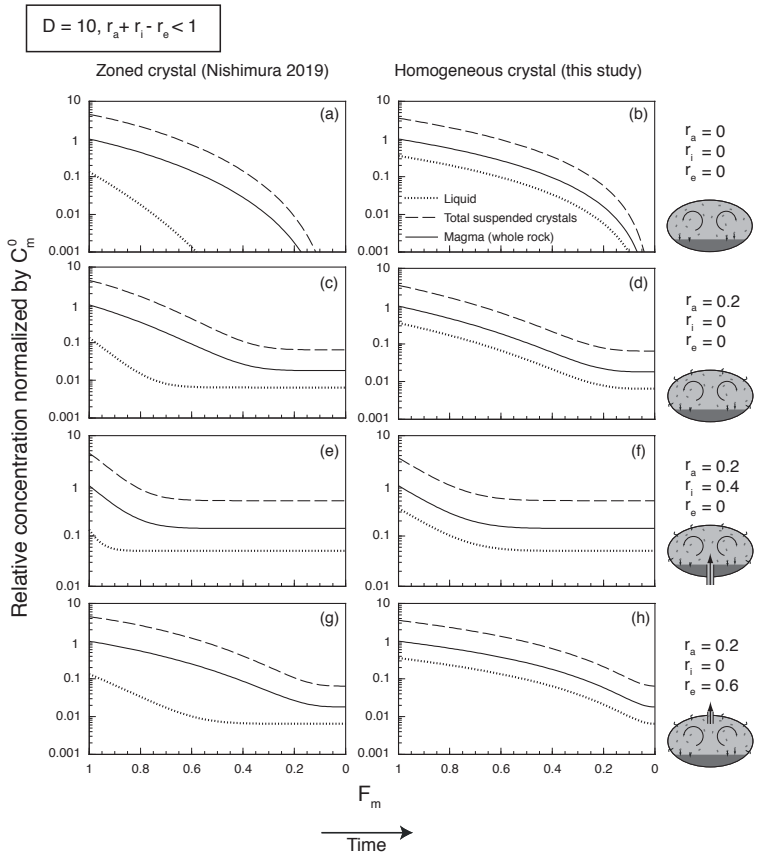

Fig. 2 : Evolution of trace element concentrations in liquid, total suspended crystals, and magma (whole rock) for the cases of zoned (left panels) and homogeneous (right panels) crystals when $D = 10$ and $r_a + r_i - r_e < 1$. Each concentration is normalized to the initial concentration in the magma, C_m^0. Trajectories are shown for $\phi = 0.2$, $C_a/C_m^0 = 0.25$, $r_a = 0.2$ and different values of r_i and r_e (see Table 1 for descriptions of the parameters).

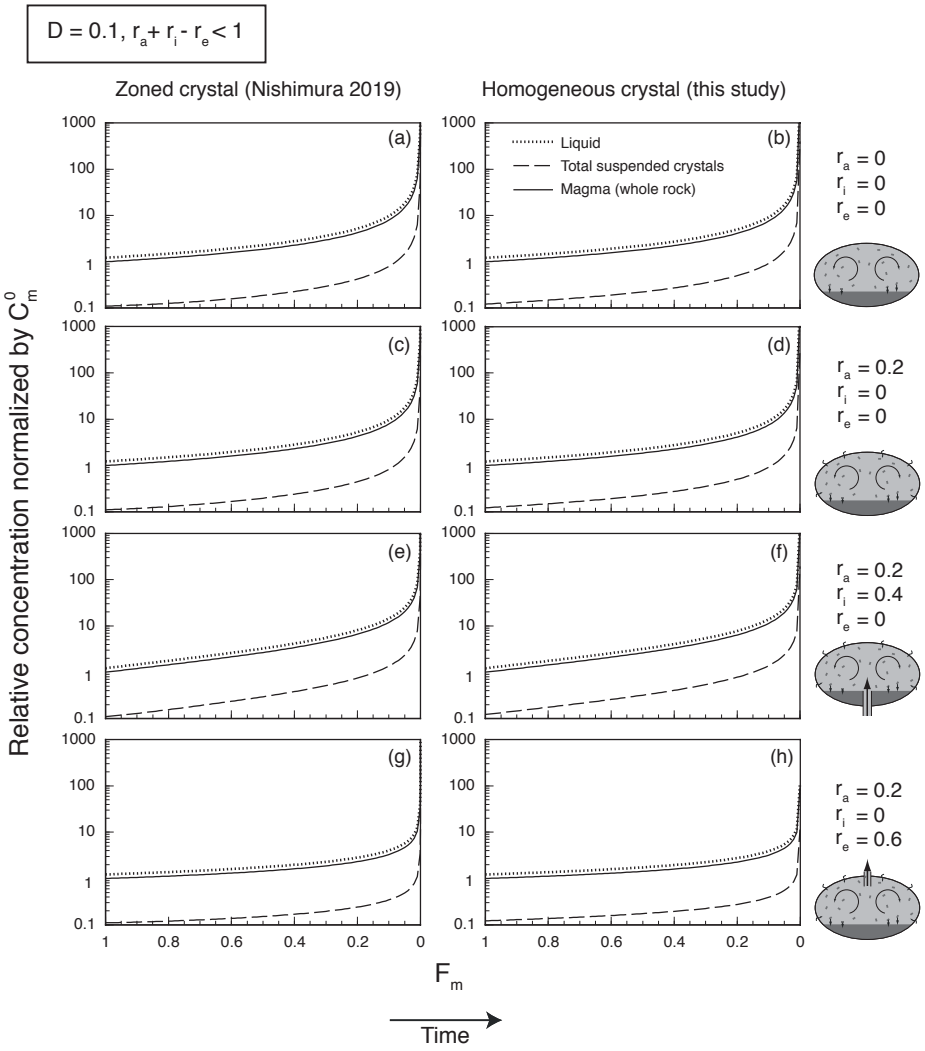

Fig. 3 : As for Fig. 2, but for D = 0.1.

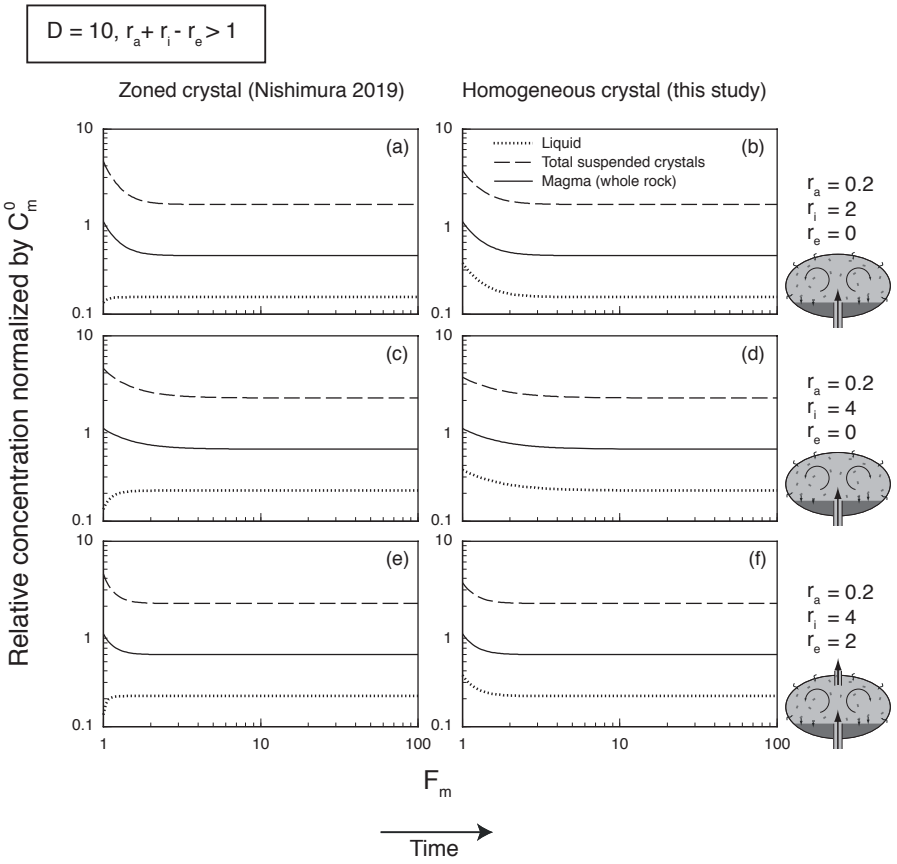

Fig. 4 : As for Fig. 2, but for $r_a + r_i - r_e > 1$.

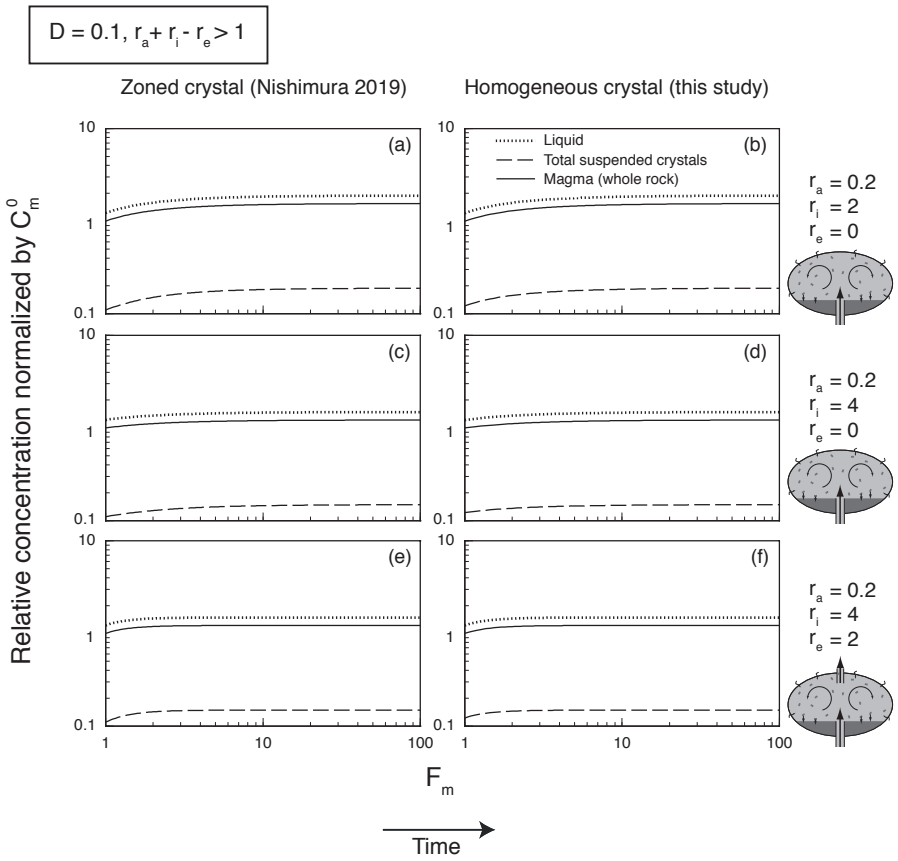

Fig. 5 : As for Fig. 2, but for D = 0.1 and $r_a + r_i - r_e > 1$.

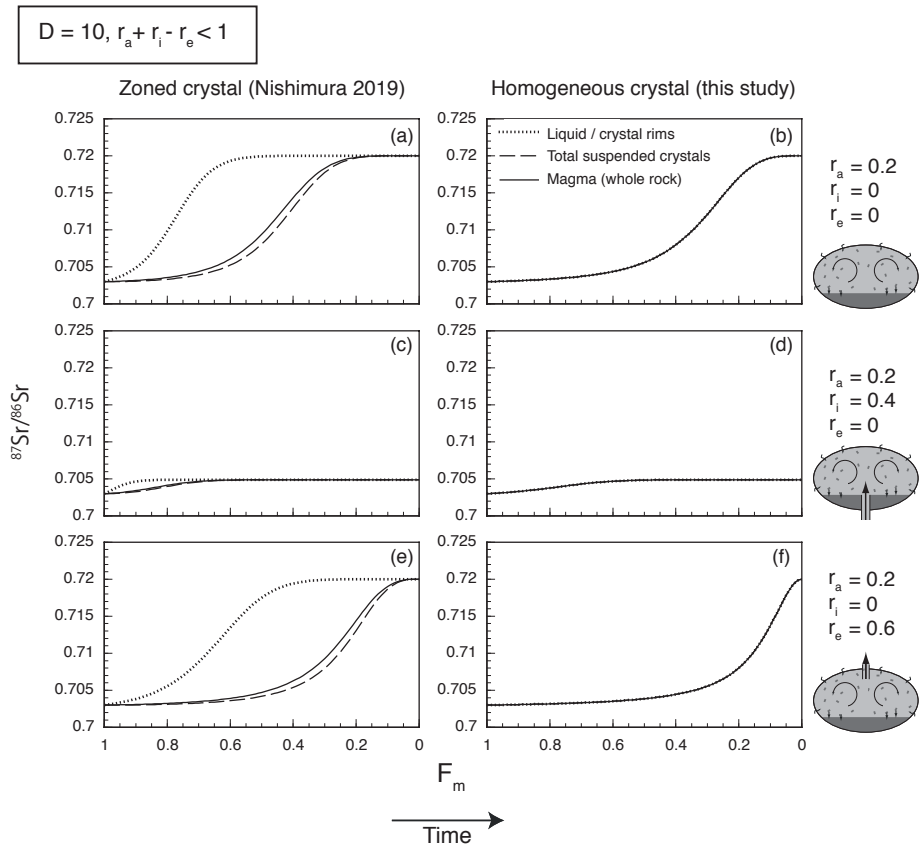

Fig. 6 : Evolution of the $^{87}Sr/^{86}Sr$ isotope ratio of liquid, crystal rims, total suspended crystals, and magma (whole rock) for the cases of zoned crystals (left panels) and homogeneous crystals (right panels) when D = 10 and $r_a + r_i - r_e < 1$. Trajectories are shown for ϕ = 0.2, C_a/C_m^0 = 0.25, r_a = 0.2, and differing values of r_i and r_e (see Table 1 for descriptions of the parameters).

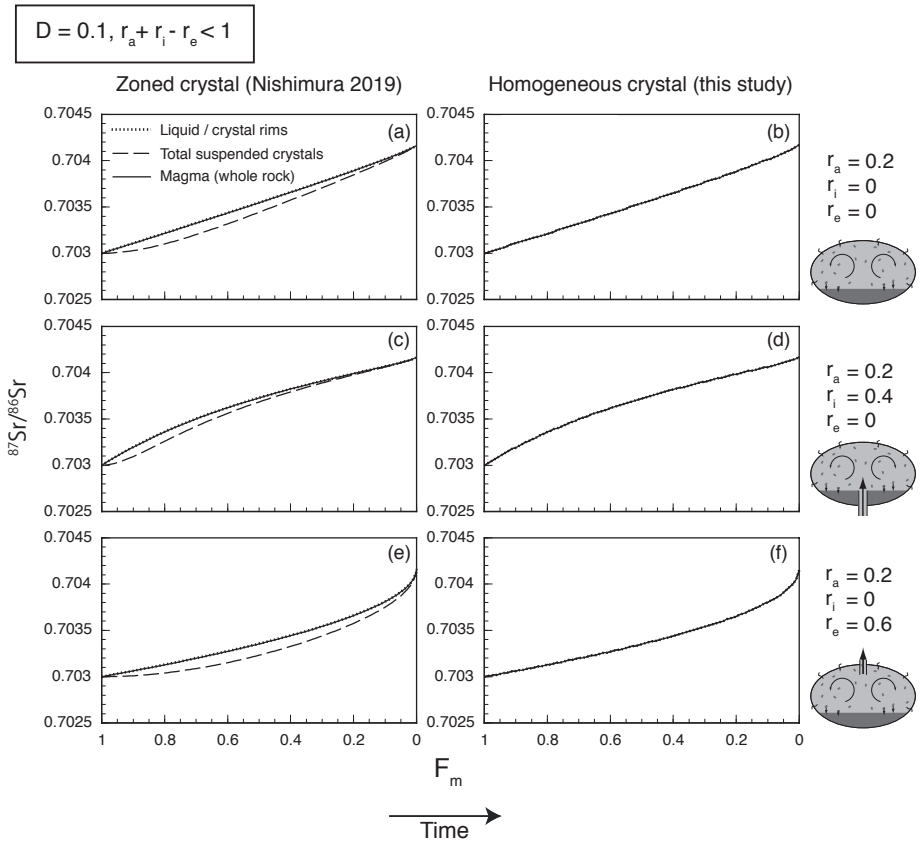

Fig. 7 : As for Fig. 6, but for D = 0.1.

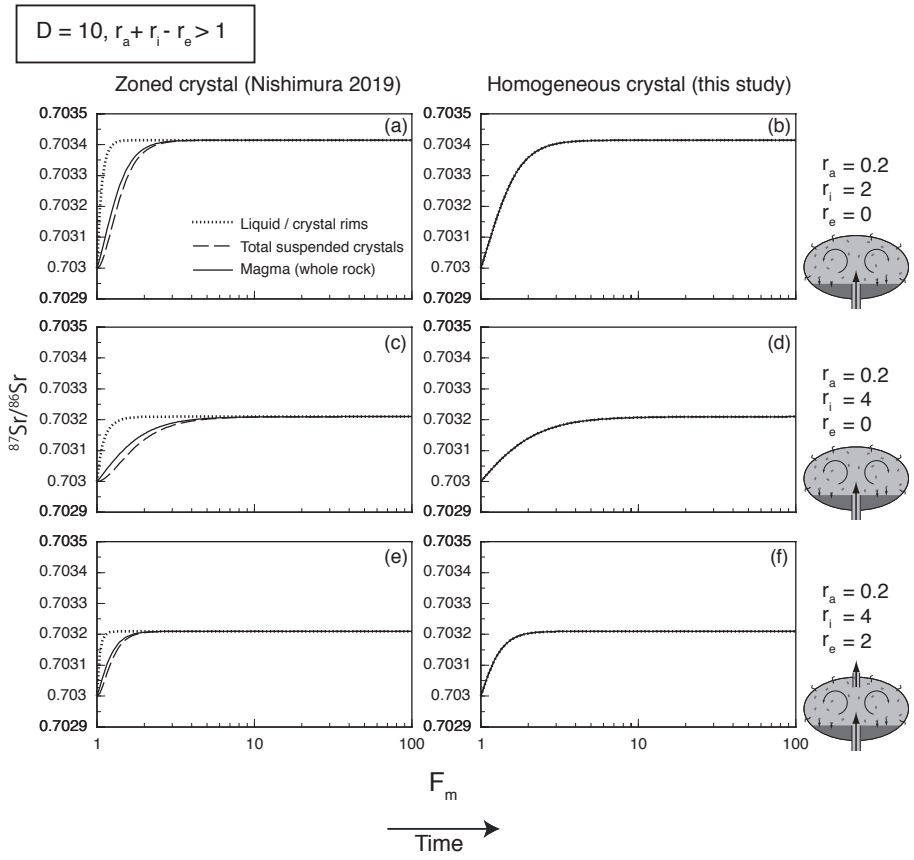

Fig. 8：As for Fig. 6, but for $r_a + r_i - r_e > 1$.

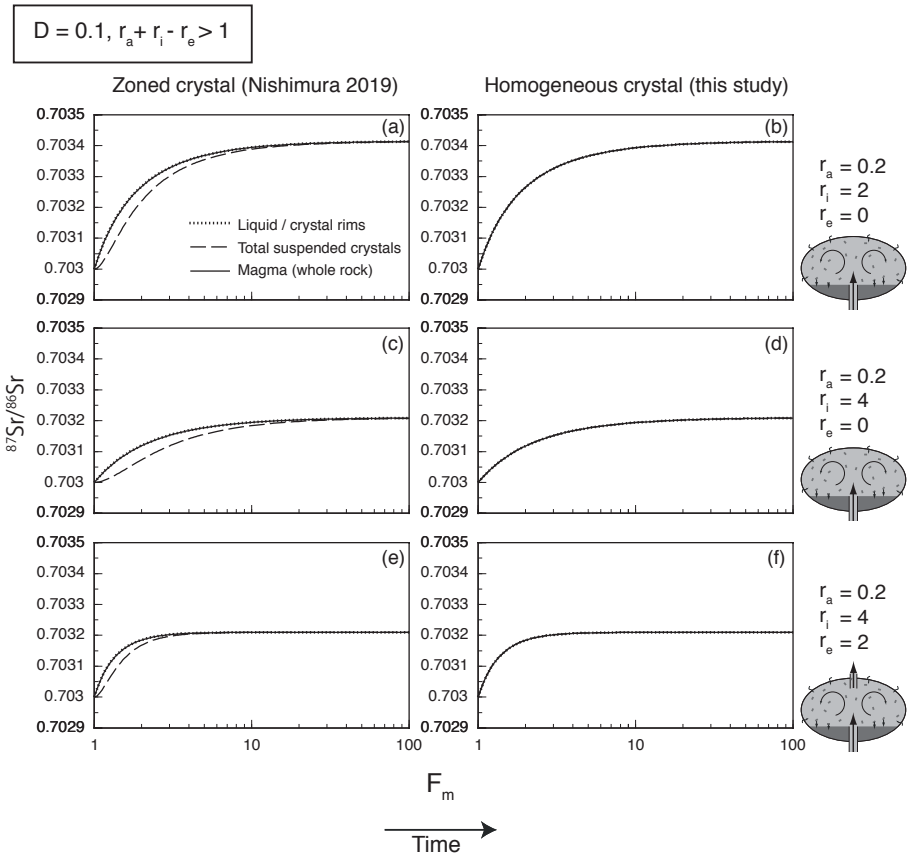

Fig. 9 : As for Fig. 6, but for D = 0.1 and $r_a + r_i - r_e > 1$.

$$C_m \approx j/k\,, \tag{19}$$

and

$$C_m \approx l/j\,. \tag{20}$$

In the case that $r_a + r_i - r_e < 1$ and D is large, k (Eq. 11) may have a negative value. In this case, F_m^{-i} in Eqs. (6)–(9) and F_m^{-k} in Eqs. (8) and (9) show rapid reductions with decreasing F_m, and the steady state compositions are described by Eqs. (19) and (20). When $r_a + r_i - r_e > 1$, then k may have a positive value regardless of D, and F_m increases as the process advances. In this case, F_m^{-k} shows a rapid reduction with increasing F_m, and the steady state compositions become identical to those described by Eqs. (19) and (20), which can also be expressed as

$$C_m \approx \frac{(r_a C_a + r_i C_i)(\phi D + 1 - \phi)}{(r_a + r_i - 1)(\phi D + 1 - \phi) + D}\,, \tag{21}$$

and

$$\varepsilon_m \approx \frac{r_a C_a \varepsilon_a + r_i C_i \varepsilon_i}{r_a C_a + r_i C_i}\,. \tag{22}$$

These steady state trace element and isotopic compositions are derived for the cases of both homogeneous and zoned crystals (Nishimura, 2019). The two end-member models (i.e., the models of this study and of Nishimura, 2019) provide upper and lower limits for the compositional variations caused by various degrees of solid-state equilibration during open-system magma chamber processes.

References

Aitcheson, S.J., Forrest, A.H., 1994. Quantification of crustal contamination in open magmatic systems. J. Petrol. 35: 461–488

Bohrson,W.A., Spera, F.J. 2001. Energy-constrained open-system magmatic processes II: Application of energy-constrained assimilation–fractional crystallization (EC-AFC) model to magmatic systems. J. Petrol. 42: 1019–1041.

Caffe, P.J., Trumbull, R.B., Coira, B.L., Romer, R.L. 2002. Petrogenesis of early Neogene magmatism in the northern Puna; implications for magma genesis and crustal processes in the central Andean Plateau. J. Petrol. 43: 907–942.

Charlier, B.L.A., Ginibre, C., Morgan, D., Nowell, G.M., Pearson, D.G., Davidson, J.P., Ottley, C.J. 2006. Methods for the microsampling and high-precision analysis of strontium and rubidium isotopes at single crystal scale for petrological and geochronologi-

cal applications. Chem. Geol. 232: 114–133.
Charlier, B.L.A., Wilson, C.J.N., Davidson, J.P. 2008. Rapid open-system assembly of a large silicic magma body: time-resolved evidence from cored plagioclase crystals in the Oruanui eruption deposits, New Zealand. Contrib. Mineral. Petrol. 156: 799–813.
Costa, F., Chakraborty, S., Dohmen, R. 2003. Diffusion coupling between trace and major elements and a model for calculation of magma residence times using plagioclase. Geochim. Cosmochim. Acta 67: 2189–2200.
Costa, F., Coogan, L.A., Chakraborty, S. 2010. The time scales of magma mixing and mingling involving primitive melts and melt–mush interaction at mid-ocean ridges. Contrib. Mineral. Petrol. 159, 371–387.
Davidson, J.P., Tepley, F.J. III 1997. Recharge in volcanic systems: evidence from isotope profiles of phenocrysts. Science 275: 826–829.
Davidson, J.P., Tepley, F.J. III, Knesel, K.M. 1998. Isotopic fingerprinting may provide insights into evolution of magmatic systems. EOS Trans Am Geophys Union 79: 185, 189, 193
Davidson, J.P., Tepley, F.J. III, Palacz, Z., Meffan-Main, S. 2001. Magma recharge, contamination and residence times revealed by in situ laser ablation isotopic analysis of feldspar in volcanic rocks. Earth Planet. Sci, Lett. 184: 427–442.
Davidson, J.P., Morgan, D.J., Charlier, B.L.A., Harlou, R., Hora, J.M. 2007. Microsampling and isotopic analysis of igneous rocks: implications for the study of magmatic systems. Ann. Rev. Earth Planet. Sci. 35: 273–311.
DePaolo, D.J. 1981. Trace element and isotopic effects of combined wallrock assimilation and fractional crystallization. Earth Planet. Sci. Lett. 53: 189–202.
Druitt, T.H., Costa, F., Deloule, E., Dungan, M., Scaillet, B. 2012. Decadal to monthly timescales of magma transfer and reservoir growth at a caldera volcano. Nature 482: 77–80.
Feldstein, S.N., Halliday, A.N., Davies, G.R., Hall, C.M. 1994. Isotope and chemical microsampling: constraints on the history of an S-type rhyolite, San Vincenzo, Tuscany, Italy. Geochim. Cosmochim. Acta 58: 943–958.
Knesel, K.M., Davidson, J.P., Duffield, W.A. 1999. Evolution of silicic magma through assimilation and subsequent recharge: evidence from Sr isotopes in sanidine phenocrysts, Taylor Creek Rhyolite, NM. J. Petrol. 40: 773–786.
Mantovani, M.S.M., Hawkesworth, C.J. 1990. An inversion approach to assimilation and fractional crystallisation processes. Contrib. Mineral. Petrol. 105: 289–302.
Martin, D., Nokes, R. 1988. Crystal settling in a vigorously convecting magma chamber. Nature 332: 534–536.

Moore A., Coogan, L.A., Costa, F., Perfit, M.R. 2014. Primitive melt replenishment and crystal-mush disaggregation in the weeks preceding the 2005–2006 eruption 9° 50 ´ N, EPR. Earth Planet. Sci. Lett. 403: 15–26.

Nishimura, K. 2009. A trace-element geochemical model for imperfect fractional crystallization associated with the development of crystal zoning. Geochim. Cosmochim. Acta 73: 2142–2149.

Nishimura, K. 2012. A mathematical model of trace element and isotopic behavior during simultaneous assimilation and imperfect fractional crystallization. Contrib. Mineral. Petrol. 164: 427–440.

Nishimura, K. 2019. Chemical mass balance equations for open-system magma chamber processes that result in crystal zoning. J. Volcanol. Geotherm. Res. 374: 181–196

O'Hara, M. J. 1993. Trace element geochemical effects of imperfect crystal-liquid separation. In Magmatic Processes and Plate Tectonics (eds. H. M. Prichard, T. Alabaster, N. B. W. Harris and C. R. Neary). Special Publication of the Geological Society, London. pp. 39–59.

O'Hara, M. J., Fry N. 1996. The highly compatible trace element paradox–fractional crystallization revisited. J. Petrol. 37: 859–890.

Powell, R. 1984. Inversion of the assimilation and fractional crystallization (AFC) equations; characterization of contaminants from isotope and trace element relationships in volcanic suites. J. Geol. Soc. London 141: 447–452.

Ramos, F.C., Wolff, J.A., Tollstrup, D.L. 2005. Sr isotope disequilibrium in Columbia River flood basalts: Evidence for rapid shallow-level open-system processes. Geology 33: 457–460.

Roberts, M.P., Clemens, J.D. 1995. Feasibility of AFC models for the petrogenesis of calk-alkaline magma series. Contrib. Mineral. Petrol. 121: 139–147.

Saunders, K.E., Morgan, D.J., Baker, J.A., Wysoczanski, R.J. 2010. The magmatic evolution of the Whakamaru supereruption, New Zealand, constrained by a microanalytical study of plagioclase and quartz. J. Petrol. 51: 2465–2488.

Singer, B.S., Costa, F., Herrin, J.S., Hildreth, W., Fierstein, J. 2016. The timing of compositionally-zoned magma reservoirs and mafic 'priming' weeks before the 1912 Novarupta-Katmai rhyolite eruption. Earth Planet. Sci. Lett. 451: 125–137.

Tepley, F.J. III, Davidson, J.P., Clynne, M.A. 1999. Magmatic interactions as recorded in plagioclase phenocrysts of Chaos Crags, Lassen Volcanic Center, California. J. Petrol. 40: 787–806.

Tepley, F.J. III, Davidson, J.P., Tilling, R.I., Arth, J.G. 2000. Magma mixing, recharge and eruption histories recorded in plagioclase phenocrysts from EL Chichón Volcano, Mexico. J. Petrol. 41: 1397–1411.

Till, C.B., Vazquez, J.A., Boyce, J.W. 2015. Months between rejuvenation and volcanic eruption at Yellowstone caldera, Wyoming. Geology 43: 695–698.

Waight, T.E., Maas, R., Nicholls, I.A. 2000. Fingerprinting feldspar phenocrysts using crystal isotopic composition stratigraphy: implications for crystal transfer and magma mingling in S-type granites. Contrib. Mineral. Petrol. 139: 227–239.

Young, E.D., Wooden, J.L., Shieh, Y-N., Farber, D. 1992. Geochemical evolution of Jurassic diorites from the Bristol Lake region, California, USA, and the role of assimilation. Contrib. Mineral. Petrol. 110: 68–86.

和文要旨

平衡結晶作用の条件下における
開放系マグマ溜まりプロセスの化学質量保存式

西 村 光 史

開放系マグマ溜まりにおけるメルトの注入（再注入または混合）、平衡結晶作用、マグマ抽出（噴火等）、母岩溶融メルトの同化、結晶の部分沈降の効果を考量した質量保存モデルを構築した。質量保存の微分方程式系を解析的に解くことにより、平衡結晶作用が生じる場合の開放系マグマ溜まりの微量元素・同位体比の進化を定量的に見積もることが可能となった。